

The Chiral Phase Transition

Thomas Schäfer^a

^aInstitute for Nuclear Theory
Department of Physics
University of Washington
Seattle, WA 98195

I review the current understanding of the chiral phase transition in QCD, with particular emphasis on recent results in the instanton liquid model.

1. Introduction

An analysis of the spectra of particles produced in heavy ion collisions at CERN and AGS indicates that the excited matter created in these reactions spends most of its life time close to the QCD phase transition [1]. Under these circumstances, we cannot expect that the phenomena observed in these collisions can be understood in terms of a perturbative plasma of quarks and gluons occupying the reaction zone. Instead, we have to address the non-perturbative aspects of QCD associated with the phase transition itself. Furthermore, it is these phenomena that can really teach us something about the structure of the QCD vacuum at zero temperature and baryon density. In this contribution, I will try to summarize our current theoretical understanding of the QCD phase transition. In particular, I will report on recent progress in understanding the chiral phase transition in the instanton liquid model.

Lattice results on the QCD phase transition are discussed in E. Laermann's contribution, and I will not go into detail here. Nevertheless, I would like to emphasize one important point. QCD has a very rich phase structure as a function of the number of colors, the number of flavors and their masses. In particular, pure gauge QCD has a first order deconfinement transition, while QCD with $N_f = 3$ massless flavors has a first order chiral transition, see figure 1. These two transitions are not connected. When the mass of the fermions is varied from $m = 0$ to $m = \infty$ (corresponding to the pure gauge theory), the two first order transitions are separated by a region in the phase diagram in which there is no true phase transition, just a rapid crossover. Indeed, the order of the phase transition for real QCD, with two light and one intermediate mass flavor is still not established with certainty.

The distinction between the pure gauge deconfinement and the light quark chiral phase transition is not just purely academic. In fact, the two transitions have completely different energy scales. The chiral phase transition takes place at $T_c \simeq 150$ MeV, while the pure gauge transition occurs at $T_c \simeq 260$ MeV (where the scale is set by the rho meson mass or the string tension). In terms of energy density (and tax dollars!), this is

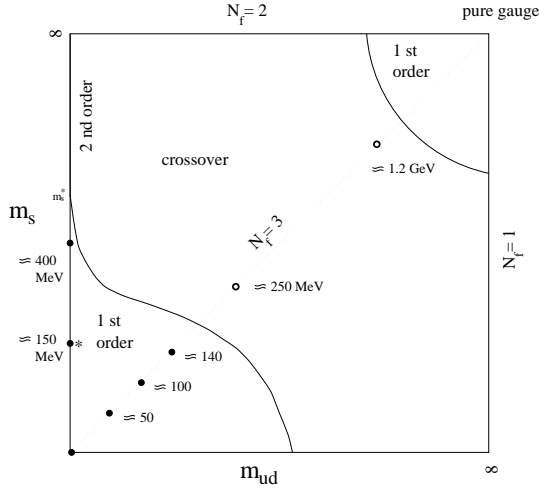


Figure 1. Schematic phase diagram for QCD in the $m_{u,d}-m_s$ plane, from [2]. The points show the type of transition found in lattice simulations with Wilson fermions. Note that QCD (*) appears to be in the first order region, while earlier simulations with staggered fermions placed QCD in the crossover region [3].

an order-of-magnitude difference. Also, the latent heat associated with the pure gauge transition is rather large, on the order of $1.5 \text{ GeV}/\text{fm}^3$, while the chiral decondensation energy is $\Delta\epsilon \simeq 250 \text{ MeV}/\text{fm}^3$. This has important consequences for the non-perturbative gluon condensate. While most of the gluon condensate is removed across the pure gauge transition, there is evidence that a significant part of it remains above the chiral transition.

2. Vacuum engineering

In Monterey T.D. Lee reminded us that the ultimate goal of relativistic heavy ion collisions is vacuum engineering, the removal of the quark and gluon condensates present in the $T = \mu = 0$ vacuum. Here in Germany, vacuum engineering has a long tradition. More than three hundred years ago Otto v. Guericke, after inventing a suitable pump, demonstrated the existence of air pressure by evacuating a pair of hollow semi-spheres. In QCD, we have to overcome the non-perturbative vacuum pressure in order to produce a perturbative vacuum state. The vacuum pressure is determined by the trace anomaly

$$p = -\frac{1}{4}\langle T_{\mu\mu} \rangle = \frac{b}{32\pi}\langle\alpha_s G^2\rangle - \frac{1}{4}\sum_f m_f\langle\bar{q}_f q_f\rangle, \quad (1)$$

where $b = 11N_c/3 - 2N_f/3$ is the first coefficient of the beta function. Using the canonical values of the condensates, this relation gives $p = 500 \text{ MeV}/\text{fm}^3$. At low temperature, the T -dependence of the condensates is determined by chiral perturbation theory [4]

$$\langle\bar{q}q\rangle = \langle\bar{q}q\rangle_0 \left\{ 1 - \frac{N_f^2 - 1}{3N_f} \left(\frac{T^2}{4f_\pi^2}\right) - \frac{N_f^2 - 1}{18N_f^2} \left(\frac{T^2}{4f_\pi^2}\right)^2 + \dots \right\}, \quad (2)$$

$$\langle\alpha_s G^2\rangle = \langle\alpha_s G^2\rangle_0 - \frac{4\pi^4}{405b} N_f^2 (N_f^2 - 1) \frac{T^8}{f_\pi^4} \left(\log\left(\frac{\Lambda}{T}\right) - \frac{1}{4} \right) - \dots \quad (3)$$

To leading order, the T -dependence of the quark condensate has a very simple interpretation in terms of the number of thermal pions times the pion matrix element of the quark condensate, $\langle\pi|\bar{q}q|\pi\rangle = -\langle\bar{q}q\rangle/f_\pi^2$ [5]. This means that pions act as a vacuum cleaner for the chiral condensate, each thermal pion removes $\sim 5 \bar{q}q$ pairs. On the other hand, the

gluon content of the pion is rather small. Naively extrapolating these results to larger temperatures, one expects chiral symmetry restoration to occur at $T \simeq 260$ MeV, while the gluon condensate is essentially T -independent. This estimate is not strongly affected by higher loop corrections in ChPTh. Clearly, chiral perturbation theory was not meant to be used near the transition. Nevertheless, the result indicates that something more than just pions is needed to restore the symmetry at the expected temperature. It also shows that even if the chiral expansion is apparently convergent, the neglected (exponentially small) terms need not be small.

The thermodynamics of the phase transition is usually described in terms of a bag model equation of state. This EOS directly incorporates the idea that the transition takes place as soon as the perturbative pressure from quarks and gluons can overcome the non-perturbative bag pressure in the QCD vacuum. For $N_f = 2$ and $B = 500 \text{ MeV}/fm^3$ from (1) this gives the estimate $T_c = [(90B)/(37\pi^2)]^{1/4} \simeq 180$ MeV. Analyzing lattice thermodynamics in more detail one finds that this estimate is too large, because only $\sim 1/2$ of the bag pressure is removed across the phase transition [6–8].

An even simpler approach to estimate the critical temperature is based on the idea that the transition occurs when thermal hadrons begin to overlap. The density of hadrons becomes of order 1 fm^{-3} near $T \simeq 200$ MeV. This is reasonably close to T_c (although, if T_c is really 150 MeV then $n_{had}(T_c) \simeq 0.15 \text{ fm}^{-3}$). Nevertheless, this kind of argument is not correct in general. A good example is pure gauge QCD, where $T_c \simeq 250$ MeV, but the lightest state is at ~ 1.7 GeV, so the particle density below T_c is small, on the order of $n \simeq 0.005 \text{ fm}^{-3}$. The lesson is that a first order transition occurs if the high T (QGP) and low T (hadronic) phases have the same free energy; the phase transition point cannot be inferred from looking at the low temperature phase only.

3. QCD near T_c

Chiral perturbation theory is based on a non-linear effective lagrangian in which the σ , the chiral partner of the pion, is eliminated. Near T_c , this description is not expected to be useful. However, in the vicinity of a second order phase transition, universality implies that critical phenomena are governed by an effective Landau-Ginzburg action for the chiral order parameter. In the case of QCD with two (massless) flavors the order parameter is a four-vector $\phi^a = (\sigma, \vec{\pi})$. Universality makes definite predictions for the critical behavior of $\langle \bar{q}q \rangle$, the chiral susceptibility and the specific heat near T_c [9–11]. At the moment, these predictions appear to be in agreement with lattice gauge results [12], but the issue has not been completely settled [13].

I would like to make a few comments concerning the role of universality arguments. First, it is important to clearly distinguish between the low energy chiral lagrangian (or the linear σ -model used as an effective lagrangian, see e.g. [14]) and the effective action for the order parameter near T_c . The Landau-Ginzburg action is a three dimensional action for static modes only. It is applicable only near T_c . In particular, the parameters in the effective action, the π, σ masses and couplings, are completely independent of the parameters used in the linear σ -model at $T = 0$. My second point concerns the thermodynamics of the phase transition. The effective action describes the singular part of the free energy only. In QCD we expect a large change in the free energy that corresponds

to the release of 37 (quark and gluon) degrees of freedom. This means that in practice, the non-universal, regular, part of the free energy will most likely dominate the universal, singular, contribution.

Universality predicts the behavior of three dimensional (screening) correlation functions near T_c . The corresponding screening masses have also been studied in some detail on the lattice, see section 5. In practice, however, we are more interested in dynamical (temporal) masses, corresponding to poles of the spectral function in energy, not momentum. These quantities are hard to extract on the lattice, although some exploratory studies have been made [15]. In addition to that, we have made significant progress in studying temporal correlation functions in the instanton liquid model (see below). The only general approach to the problem that we have available at the moment are QCD sum rules.

The general strategy is easily explained. It is based on matching phenomenological information contained in hadronic spectral function with perturbative QCD, using the operator product expansion. At finite temperature, the sum rules are of the type

$$c_0 \log \omega^2 + c_1 \langle O_1 \rangle \frac{1}{\omega^4} + c_2 \langle O_2 \rangle \frac{1}{\omega^6} + \dots = \int du^2 \frac{\rho(u^2)}{u^2 - \omega^2}, \quad (4)$$

where $\rho(\omega^2)$ is the spectral function at $\vec{p} = 0$, c_i are temperature independent coefficients that can be calculated in perturbative QCD and $\langle O_i \rangle$ are temperature dependent condensates. If there is a range in energies in which both the OPE has reasonable accuracy and the spectral representation is dominated by the ground state, we can use the sum rules to make predictions about ground state properties.

In practice, this is a difficult game, even at zero temperature. At $T \neq 0$, additional problems arise because we do not know the T -dependence of the condensates and there is little phenomenological guidance concerning the form of the spectral functions. For this reason, reliable predictions can only be made at small temperature. The most systematic studies have been made in the vector meson channels ρ and a_1 [16–18]. To order T^2 , there is no shift in the resonance masses. The only effect is mixing between the ρ and a_1 channels, which is caused by scattering off thermal pions. At order T^4 , masses start to drop. It is interesting to note that at this order, the mass shift is not controlled by the quark condensate, but the energy momentum tensor in a thermal pion gas.

4. The instanton liquid at finite temperature

In order to make progress we need a more detailed picture of the chiral phase transition. In particular, we would like to understand the mechanism of the transition and the behavior of the condensates and hadronic correlation functions in the transition region. In the following, I will argue that important progress in this direction has been made in the context of the instanton liquid model. In this model, chiral symmetry breaking is caused by the delocalization of quark zero modes associated with instantons. Chiral restoration takes place when instantons and antiinstantons form molecules, the quark modes become localized and the quark condensate is zero.

The essential assumption underlying the instanton model is that the (euclidean) QCD

partition function

$$Z = \int DA_\mu \exp(-S) \prod_f^{N_f} \det(i\mathcal{D} + im_f), \quad (5)$$

is dominated by classical gauge configurations called instantons. Instantons describe tunneling events between degenerate vacua. As usual, tunneling lowers the ground state energy. This is why instantons contribute to the vacuum energy density and pressure in the QCD vacuum. The instanton solution is characterized by 12 parameters, position (4), color orientation (7) and size (1). An ensemble of interacting instantons is described by the partition function

$$Z = \sum_{N_+N_-} \frac{1}{N_+!N_-!} \int \prod_i^{N_++N_-} [d^4z_i dU_i d\rho_i d(\rho_i)] \exp(-S_{int}) \prod_f^{N_f} \det(i\mathcal{D} + im_f), \quad (6)$$

where N_+ and N_- are the numbers of instantons and antiinstantons and $d(\rho)$ is the semi-classical instanton density calculated by 't Hooft. There are two important pieces of evidence that suggest that instantons play an important role in the QCD vacuum. One is provided by extensive calculations of hadronic correlation functions in the instanton liquid model [19–21]. These correlators agree both with phenomenological information [22] and lattice calculations [23]. The second comes from direct studies of instantons on the lattice. An example is shown in figure 2. Using a procedure called “cooling” one can relax any given gauge field configuration to the closest classical component of the QCD vacuum. These configurations were found to be ensembles of instantons and antiinstantons. The MIT group concludes that the instanton density is $(N/V) \simeq (1.4 - 1.6) \text{ fm}^{-4}$ while the typical size is about $\rho \simeq 0.35 \text{ fm}$ [24]. These numbers are in good agreement with the instanton liquid parameters $(N/V) = 1 \text{ fm}^{-4}$, $\rho = 1/3 \text{ fm}$ proposed by Shuryak a long time ago [25]. What is even more important is that hadronic correlation functions remain practically unchanged during the cooling process. This suggests that instantons play a dominant role in generating the spectrum of light hadrons.

Recently, the role of instantons at finite temperature has been reevaluated. The semi-classical expression for the instanton density at finite temperature contains a suppression factor $\sim \exp(-(2N_c/3 + N_f/3)(\pi\rho T)^2)$ [26] which comes mostly from Debye screening of the instanton field. From this expression we would expect that instantons are significantly suppressed (~ 0.2) near T_c . This is not correct. The perturbative expression for the Debye mass is not applicable until the temperature is significantly above T_c . We have already seen that the gluon condensate is essentially temperature independent at small T . A similar calculation can also be performed for the instanton density, with the same conclusion [27]. This result was confirmed in a number of lattice calculations (in quenched QCD) [28–30], see figure 3. The figure shows the topological susceptibility which, in quenched QCD, is roughly equal to the instanton density. The Pisarski-Yaffe prediction (labeled P-Y) clearly underpredicts the topological susceptibility near T_c . The dashed curve which fits the data above T_c corresponds to the PY-prediction with a shifted temperature $T \rightarrow (T - T_c)$.

If instantons are not suppressed around T_c , then the chiral phase transition has to be caused by a rearrangement of the instanton liquid. A mechanism for such a rearrangement, the formation of polarized instanton-antiinstanton molecules, was proposed in [31,32]. In

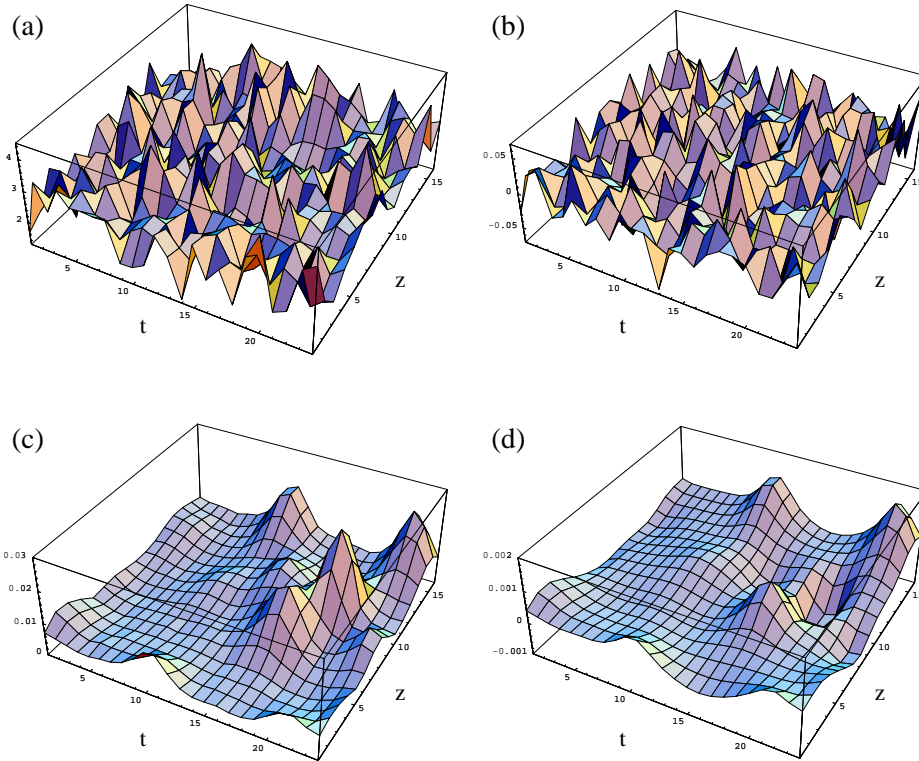


Figure 2. Instanton content of a typical $T = 0$ gauge configuration, from [24]. Figs. (a) and (c) show the field strength while (b) and (d) show the topological charge density. The upper panel shows the original configuration and the lower panel the same configuration after 25 cooling sweeps.

the presence of light fermions, instantons interact via the exchange of $2N_f$ quarks (see fig. 4). The amount of correlations in the instanton ensemble depends on the competition between maximum entropy, which favors randomness, and minimum action, which favors the formation of instanton anti-instanton pairs. At low temperatures the instanton system is random and chiral symmetry is broken. At high temperatures the interaction in the spacelike direction becomes screened, whereas the periodicity of the fields in the timelike interaction causes the interaction in that direction to be enhanced. Schematically, the fermion determinant for one pair looks like

$$\det(i\mathcal{D}) \sim |\sin(\pi T\tau)/\cosh(\pi Tr)|^{2N_f}, \quad (7)$$

where τ and r are the separations in the temporal and spatial direction. This interaction is maximal for $r = 0$ and $\tau = \beta/2 = (1/2T)$ which is the most symmetric configuration of the $I\bar{I}$ pair on the Matsubara torus.

In numerical simulations, we find the transition to a correlated system in which chiral symmetry is restored at $T_c \simeq 130$ MeV [33]. Typical instanton configurations below and above T_c are shown in figure 5. The plots are projections of a four dimensional box

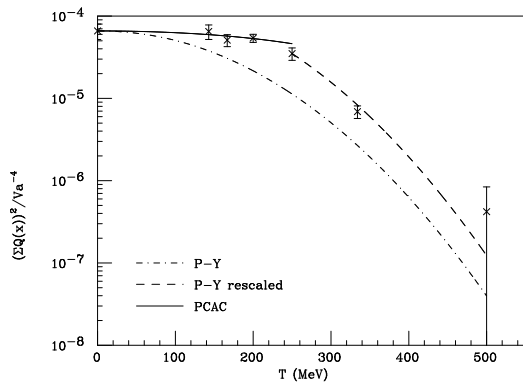


Figure 3. χ_{top} as a function of temperature in quenched QCD, from [28].

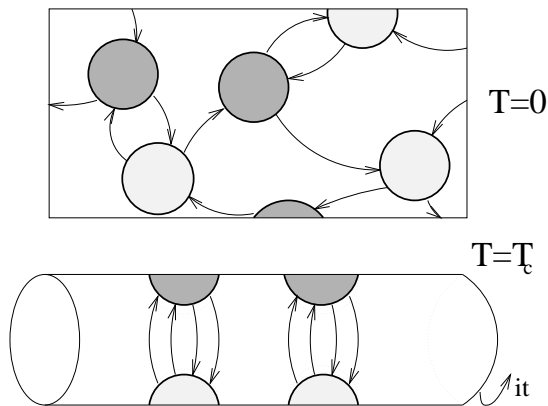


Figure 4. Schematic picture of the phase transition in the interacting instanton liquid.

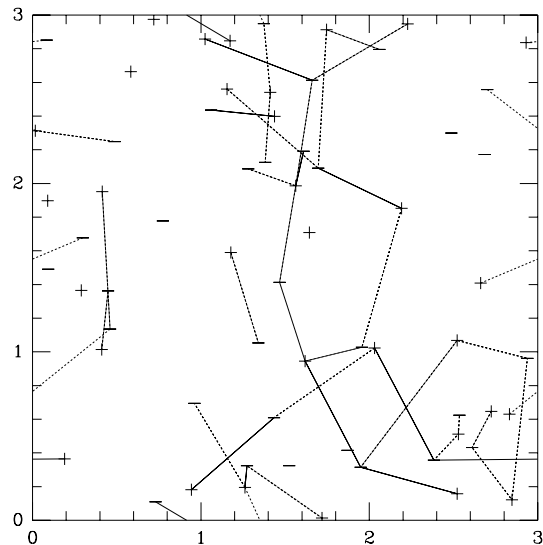


Figure 5. Instanton configurations below and above the phase transition.

into the $x\tau$ -plane. At high temperature, the imaginary time axis is short. The location of instantons and antiinstantons is denoted by \pm signs, while the lines connecting them indicate the strength of the fermionic “hopping” matrix elements. Below T_c , there is no clear pattern. Instantons are either isolated or part of larger clusters. Following the hopping matrix elements, quarks can propagate over large distances and form a condensate. Above T_c , instantons are bound into pairs. The propagation of quarks in the spatial direction is suppressed and no condensate is formed.

More details are provided in figure 6. The quark condensate is practically T -independent at small temperature, but drops rapidly above $T = 100$ MeV. At small T , the instanton density rises slightly¹. It drops above $T = 100$ MeV, but retains about half of its $T = 0$ value near T_c . Similarly, the instanton related free energy² does not vanish at T_c . Instantons still contribute to the energy density and pressure above T_c .

¹This might very well be an artefact. The $T = 0$ point is not a true zero temperature calculation.

²Figure 6b only shows the instanton-related part of the free energy, the full free energy $F = -p$ has to be a monotonically decreasing function of T .

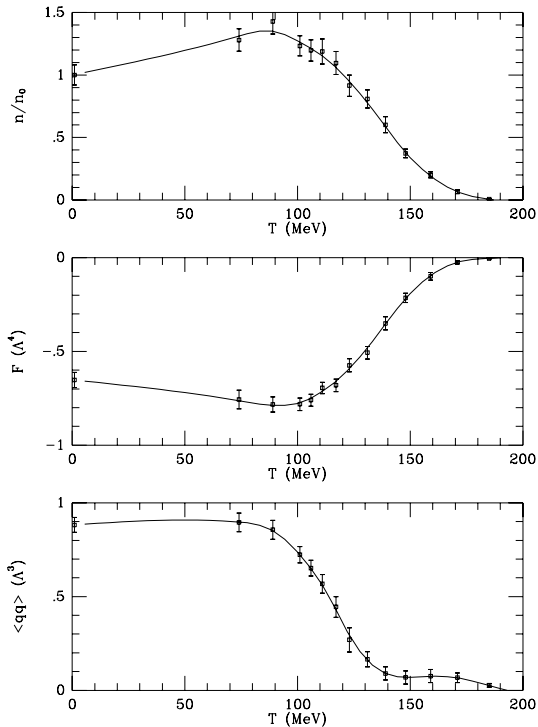


Figure 6. Instanton density, free energy and quark condensate as a function of T .

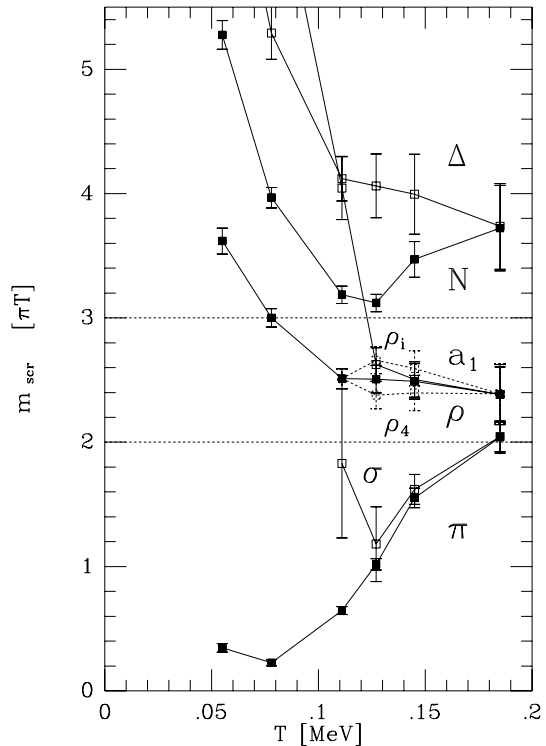


Figure 7. Screening masses in the instanton liquid model.

It is interesting to study the phase diagram in more detail. For realistic QCD, the transition appears to be weakly first order (the discontinuity in the free energy is smoothed out in a finite volume and cannot be seen in figure 6). In the case of two flavors, we see a second order phase transition with critical exponents consistent with the $O(4)$ universality class. For more flavors, the transition temperature drops until (around $N_f = 5$ massless flavors) chiral symmetry is restored in the ground state even at $T = 0$.

5. Hot hadrons

We have studied both temporal (related to the spectral function in energy) and spatial (related to screening masses) correlation functions at finite temperature [21]. Figure 7 shows the spectrum of spacelike screening masses. First, we clearly observe that chiral symmetry is restored at $T \simeq 130$ MeV. Chiral partners, like the (π, σ) and (ρ, a_1) become degenerate at T_c . Second, even above T_c , the scalars π and σ are significantly lighter than the vectors ρ and a_1 . This result is in agreement with lattice calculations [34,35]. The spectrum of screening masses is also in qualitative agreement with the predictions from dimensional reduction (DR) [36–38], but DR fails to account for the attraction seen in the scalar channels.

More interesting is the behavior of temporal correlation functions, shown in figure 8. The correlation functions are normalized to free quark propagation at the same tempera-

ture, so all correlators start at 1 for $\tau = 0$. Below T_c , the data points are denoted by open squares ($T = 0$), pentagons, etc., while the high temperature points are denoted by solid squares and pentagons. Above T_c , the period of the correlation functions becomes short, $\beta = T_c^{-1} \sim 1.5$ fm. This means that all the spectral information is contained in a very short interval $0 < \tau < \beta/2 \sim 0.7$ fm. This fact makes it very difficult to extract thermal masses from the correlation functions (or to decide whether there are narrow poles in the spectral function at all).

Again, we observe that above T_c the correlation functions of chiral partners become equal. What is more remarkable is the fact that in the regime $\tau < (\beta/2)$, which is not (directly) affected by the periodic boundary conditions, the pion³ correlation function is almost as large as it is at $T = 0$. This suggest that there is still a (π, σ) -mode above T_c [39,40]. No such effect is seen in the vector channels. The small resonance contribution seen in the ρ channel at small temperature quickly melts and above T_c the correlation function is consistent with the propagation of two independent quarks with a small residual chiral mass (a mass term in the vector part of the propagator that does not violate chiral symmetry).

What effect causes the resonance behavior seen in the scalar channels? At zero temperature, the instanton induced interaction between quarks is conveniently discussed in terms of an effective four fermion interaction⁴ [41,42]

$$\mathcal{L} = \int d(\rho)d\rho \frac{(2\pi\rho)^4}{8(N_c^2 - 1)} \left\{ \frac{2N_c - 1}{2N_c} [(\bar{\psi}\tau_a^-\psi)^2 + (\bar{\psi}\tau_a^-\gamma_5\psi)^2] - \frac{1}{4N_c} (\bar{\psi}\tau_a^-\sigma_{\mu\nu}\psi)^2 \right\}, \quad (8)$$

where $d(\rho)$ denotes the density of instantons. Here, ψ is an isodoublet of quark fields and the four vector τ_a^- has components $(\vec{\tau}, i)$ with $\vec{\tau}$ equal to the Pauli matrices acting in isospace. The interaction (8) successfully explains many properties of the ($T=0$) QCD correlation functions, most importantly the strong attraction seen in the pion channel.

The effective lagrangian (8) comes from the $2N_f$ zero modes associated with an individual instanton. It is derived under the assumptions that instantons are sufficiently dilute and completely uncorrelated. Above T_c , the collective coordinates of instantons and antiinstantons are no longer random, but become strongly correlated. The four fermion interaction induced by polarized instanton-antiinstanton molecules is given by [32]

$$\begin{aligned} \mathcal{L}_{mol\ sym} = & G \left\{ \frac{2}{N_c^2} [(\bar{\psi}\tau^a\psi)^2 - (\bar{\psi}\tau^a\gamma_5\psi)^2] \right. \\ & \left. - \frac{1}{2N_c^2} [(\bar{\psi}\tau^a\gamma_\mu\psi)^2 + (\bar{\psi}\tau^a\gamma_\mu\gamma_5\psi)^2] + \frac{2}{N_c^2} (\bar{\psi}\gamma_\mu\gamma_5\psi)^2 \right\} + \mathcal{L}_8, \quad (9) \end{aligned}$$

where the coupling constant G is determined by the number of correlated pairs (and their overlap matrix element) and \mathcal{L}_8 is the color octet part of the interaction. G is not strong enough in order to cause quarks to condense. Nevertheless, molecules produce a significant attractive interaction in the π and σ channels.

³ The σ correlation is even larger than the π below T_c because it receives a disconnected contribution from the quark condensate.

⁴Strictly speaking, a flavor antisymmetric $2N_f$ fermion interaction. However, for $N_f = 3$ and broken chiral symmetry (either spontaneous or explicit), we can absorb two zero modes into the instanton density.

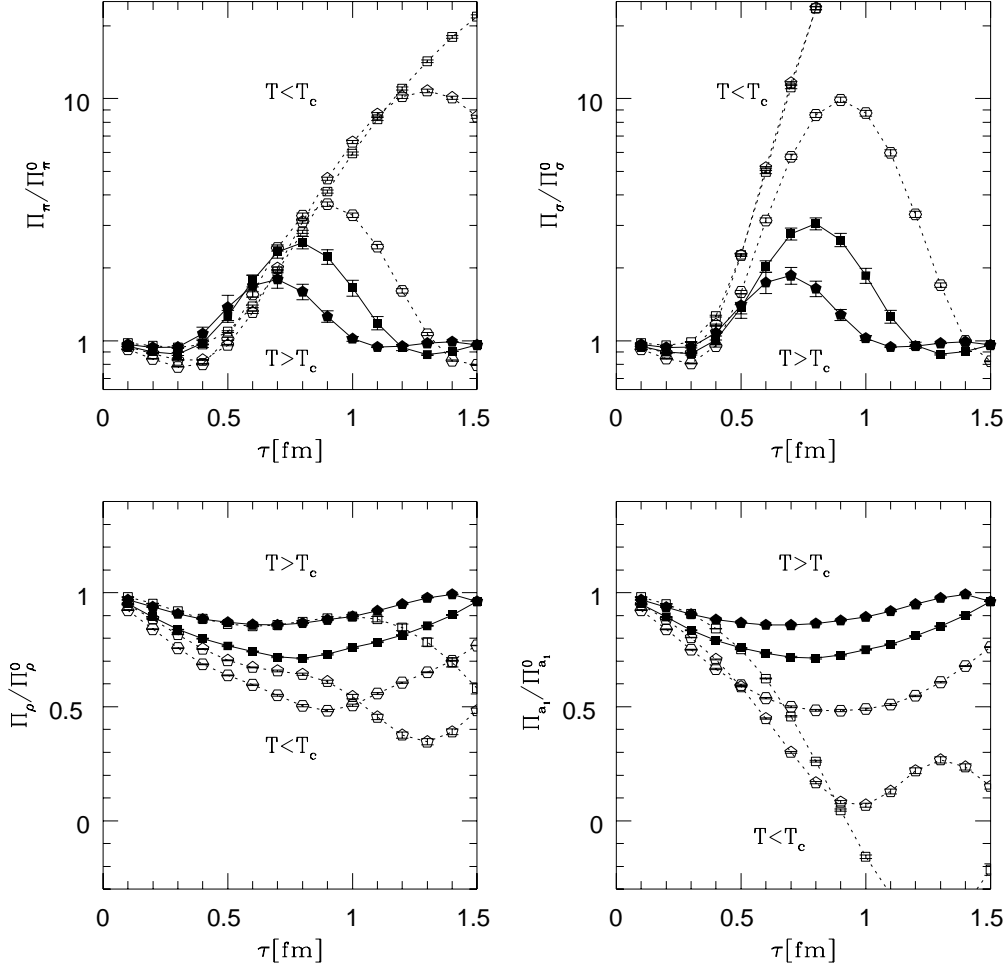


Figure 8. Temporal correlation functions in the instanton liquid model.

A problem that has received a lot of attention recently is the fate of the $U(1)_A$ anomaly at finite temperature [43–48]. Given the large $\eta' - \pi$ splitting any tendency towards $U(1)_A$ could lead to rather dramatic effects in heavy ion collisions. Two experimental signatures that have been discussed are the η/π ratio [45] measured by the WA80 collaboration [49] and the possibility that the η' Dalitz decay [44] contributes to the enhancement in low mass dileptons seen by CERES [50].

The anomaly is related to the presence of zero modes in the spectrum of the Dirac operator. Instantons can absorb N_f left handed quarks of different flavors and turn them into right handed quarks, violating axial charge by $2N_f$ units. This is the process described by the 't Hooft vertex (8). Inserting the 't Hooft interaction into the η' correlation function splits the η' from the pion⁵. Above T_c isolated instantons disappear and

⁵In QCD, flavor symmetry is broken and part of the splitting comes from the strange quark mass. However, in the absence of the anomaly we would expect the $\eta - \eta'$ mixing to be almost ideal (similar to the $\rho - \phi$ system). In this case, there is a non-strange η which is almost degenerate with the π .

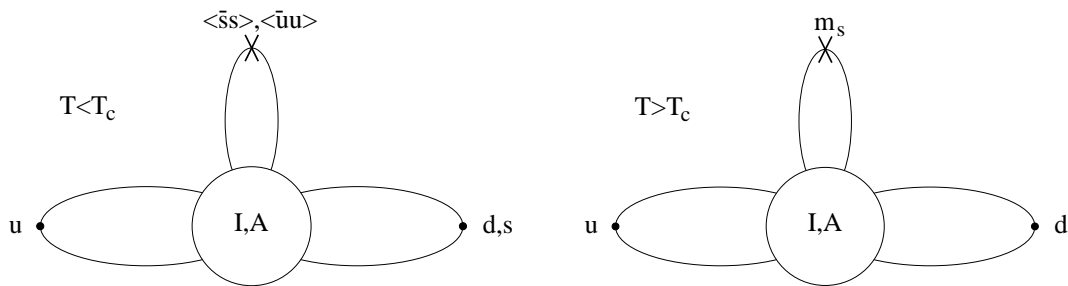


Figure 9. Flavor mixing in the $\eta - \eta'$ system below and above the chiral phase transition.

instanton-antiinstanton molecules do not violate $U(1)_A$. However, the 't Hooft operator can induce a tunneling event (instanton) all by itself. This can be seen as follows. If we keep a small current quark mass, the density of isolated instantons above T_c is proportional to m^{N_f} . When we calculate a $U(1)_A$ violating observable, there are N_f propagators⁶, each of which has a zero mode contributing a factor $1/m_f$. As a result, $U(1)_A$ is broken in the chiral limit $m_f \rightarrow 0$.

At temperatures significantly above T_c , we expect screening to reduce the strength of the $U(1)_A$ violating interaction. Near T_c , screening is not important but chiral symmetry restoration affects the structure of flavor mixing in the $\eta - \eta'$ system [51], see figure 9. Below T_c , there is strong flavor mixing between u, d and s quarks. Flavor symmetry is broken, $\langle \bar{u}u \rangle \neq \langle \bar{s}s \rangle$, but the η' state is almost pure singlet. Above T_c , there is no flavor mixing between non-strange and strange quarks. As a result, the eigenstates in the $\eta - \eta'$ system are the non-strange and strange eta components η_{NS} and η_S . The anomaly acts only on the non-strange η_{NS} , so the strange η_S can become light. This effect is of phenomenological interest, because it might enhance strangeness production in heavy ion collisions.

6. Summary

There is substantial evidence that non-perturbative effects are important in QCD, even above the phase transition. This evidence comes from an analysis of lattice results for the equation of state, the spectrum of screening masses and temporal correlation functions above T_c . This suggests that in order to understand the transition region we need a more detailed picture of the transition itself.

We have shown that the chiral phase transition can be understood as a transition from a disordered instanton liquid to a correlated phase of instanton-antiinstanton molecules. This picture is consistent with both the observation that not all of the gluon condensate is removed across the phase transition and with the observed spectrum of screening masses. It provides interesting predictions for the behavior of hadronic modes near T_c . For example, we suggest that (π, σ) -like modes survive the phase transition and that the structure

⁶In the (academic) case of three massless flavors, $U_A(1)$ violation does not affect the η' correlation function above T_c because the third quark in the 't Hooft vertex cannot be absorbed. In real QCD, the strange quark can be absorbed by a mass insertion.

of flavor mixing in the $\eta - \eta'$ sector changes near T_c .

7. Acknowledgements

The material presented here is based on work done in collaboration with E. Shuryak and J. Verbaarschot. I would also like to acknowledge many discussions with G. E. Brown, V. Koch and R. Venugopalan.

REFERENCES

1. J. Stachel. these proceedings.
2. Y. Iwasaki, K. Kanaya, S. Kaya, S. Sakai, and T. Yoshie. *Z. Phys.*, C71:343, 1996.
3. F. R. Brown, F. P. Butler, H. Chen, N. H. Christ Z.-H. Dong, W. Schaffer, L. I. Unger, and A. Vaccarino. *Phys. Rev. Lett.*, 65:2491, 1990.
4. H. Leutwyler. these proceedings.
5. J. Gasser and H. Leutwyler. *Phys. Lett.*, B184:83, 1987.
6. Y. Deng. *Nucl. Phys. (Proc. Suppl.)*, B9:334, 1989.
7. C. Adami, T. Hatsuda, and I. Zahed. *Phys. Rev.*, D43:921, 1991.
8. V. Koch and G. E. Brown. *Nucl. Phys.*, A560:345, 1993.
9. R. D. Pisarski and F. Wilczek. *Phys. Rev.*, D29:338, 1984.
10. F. Wilczek. *Int. J. Mod. Phys.*, A7:3911, 1992.
11. K. Rajagopal and F. Wilczek. *Nucl. Phys.*, B399:395, 1993.
12. F. Karsch and E. Laermann. *Phys. Rev.*, D50:6954, 1994.
13. A. Kocic and J. Kogut. *Phys. Rev. Lett.*, 74:3109, 1995.
14. A. Bokharev and J. Kapusta, 1996. *Phys. Rev. D*, to appear.
15. G. Boyd, S. Gupta, F. Karsch, and E. Laerman. *Z. Phys.*, C64:331, 1994.
16. V. L. Eletskii and B. L. Ioffe. *Phys. Rev.*, D47:3083, 1993.
17. V. L. Eletskii and B. L. Ioffe. *Phys. Rev.*, D51:2371, 1995.
18. T. Hatsuda, Y. Koike, and S. H. Lee. *Nucl. Phys.*, B394:221, 1993.
19. E. V. Shuryak and J. J. M. Verbaarschot. *Nucl. Phys.*, B410:55, 1993.
20. T. Schäfer, E. V. Shuryak, and J. J. M. Verbaarschot. *Nucl. Phys.*, B412:143, 1994.
21. T. Schäfer and E. V. Shuryak. *Phys. Rev.*, D54:1099, 1996.
22. E. V. Shuryak. *Rev. Mod. Phys.*, 65:1, 1993.
23. M. C. Chu, J. M. Grandy, S. Huang, and J. W. Negele. *Phys. Rev.*, D 48:3340, 1993.
24. M. C. Chu, J. M. Grandy, S. Huang, and J. W. Negele. *Phys. Rev.*, D49:6039, 1994.
25. E. V. Shuryak. *Nucl. Phys.*, B203:93, 1982.
26. D. J. Gross, R. D. Pisarski, and L. G. Yaffe. *Rev. Mod. Phys.*, 53:43, 1981.
27. E. V. Shuryak and M. Velkovsky. *Phys. Rev.*, D50:3323, 1994.
28. M. C. Chu and S. Schramm. *Phys. Rev.*, D51:4580, 1995.
29. E.-M. Ilgenfritz, M. Müller-Preußker, and E. Meggiolaro. *Nucl. Phys. (Proc. Suppl.)*, B42:496, 1995.
30. B. Alles, M. D'Elia, and A. Di Giacomo, 1996. hep-lat/9605013.
31. E.-M. Ilgenfritz and E. V. Shuryak. *Phys. Lett.*, B325:263, 1994.
32. T. Schäfer, E. V. Shuryak, and J. J. M. Verbaarschot. *Phys. Rev.*, D51:1267, 1995.
33. T. Schäfer and E. V. Shuryak. *Phys. Rev.*, D53:6522, 1996.
34. C. De Tar and J. Kogut. *Phys. Rev.*, D36:2828, 1987.

35. A. Gocksch. *Phys. Rev. Lett.*, 67:1701, 1991.
36. V. L. Eletsky and B. L. Ioffe. *Sov. J. Nucl. Phys.*, 48:384, 1988.
37. T. H. Hansson and I. Zahed. *Nucl. Phys.*, B374:277, 1992.
38. V. Koch, E. V. Shuryak, G. E. Brown, and A. D. Jackson. *Phys. Rev.*, D46:3169, 1992.
39. T. Hatsuda and T. Kunihiro. *Phys. Rev. Lett.*, 55:158, 1985.
40. T. Schäfer and E. V. Shuryak. *Phys. Lett.*, B356:147, 1995.
41. G. 't Hooft. *Phys. Rev.*, D14:3432, 1976.
42. M.A. Shifman, A.I. Vainshtein, and V.I. Zakharov. *Nucl.Phys.*, B163:46, 1980.
43. E. V. Shuryak. *Comm. Nucl. Part. Phys.*, 21:235, 1994.
44. J. Kapusta, D. Kharzeev, and L. McLerran. *Phys. Rev.*, D53:5028, 1996.
45. Z. Huang and X.-N. Wang. *Phys. Rev.*, D53:5034, 1996.
46. T. D. Cohen. *Phys. Rev.*, D54:1867, 1996.
47. S. H. Lee and T. Hatsuda. *Phys. Rev.*, D54:1871, 1996.
48. N. Evans, S. D. H. Hsu, and M. Schwetz. *Phys. Lett.*, B375:262, 1996.
49. WA80 collaboration: A. Lebedev et al. *Nuc. Phys.*, A566:355c, 1994.
50. Ceres collaboration: G. Agakiechev et al. *Phys. Rev. Lett.*, 75:1272, 1995.
51. T. Schäfer. in preparation.